PORTUGALIAE MATHEMATICA
Vol. 58 Fasc. 4 – 2001
Nova Série

# PATH FORMULATION FOR A MODAL FAMILY

M. Aguiar, S. Castro and I. Labouriau

**Abstract:** Persistent bifurcation diagrams in unfoldings of the modal family $g(x,\lambda) = \varepsilon\, x^4 + 2\, a\, x^2\, \lambda + \delta\, \lambda^2$ are described using path formulation: each bifurcation problem in the unfoldings of $g$ is reinterpreted as a $\lambda$-parametrized path in the universal unfolding of $x^4$. The space of unfolding parameters for the modal family is divided into regions where bifurcation problems are contact-equivalent and the bifurcation diagrams for these persistent problems are shown.

## 1 – Introduction

In bifurcation problems small perturbations in auxiliary parameters can give rise to drastic changes in bifurcation diagrams.

Given the modal family of one parameter bifurcation problems

$$g(x,\lambda) \;=\; \varepsilon\, x^4 + 2\, a\, x^2\, \lambda + \delta\, \lambda^2 \;, \tag{1}$$

where $\epsilon, \delta = \pm 1$ and the modal parameter $a$ satisfies $a^2 \neq \varepsilon\, \delta$, and given a versal unfolding of $g$ we want to enumerate, up to equivalence, the bifurcation diagrams in that unfolding.

*Received*: March 27, 2000; *Revised*: February 1, 2001.
*AMS Subject Classification*: 34D10, 58F14.
*Keywords*: Bifurcation; Path Formulation; Singularities.

In this work we use the notation of Golubitsky and Schaeffer [2]. The form of a versal unfolding of this modal family is given by Keyfitz in [3]. Among the possible versal unfoldings we choose:

$$G(x,\lambda,\tilde{a},\alpha_1,\alpha_2,\alpha_3,\alpha_4) = \\ = \varepsilon\, x^4 + 2\,\tilde{a}\, x^2\,\lambda + \delta\,\lambda^2 + \alpha_1 + \alpha_2\, x + \alpha_3\, x^2 + \alpha_4\, x\,\lambda\ , \tag{2}$$

where $(x,\lambda,\tilde{a},\alpha_1,\alpha_2,\alpha_3,\alpha_4)$ varies in a neighbourhood of $(0,0,a,0,0,0,0)$. For most values of $a$ (all except a finite number) the topological type of the problem is independent of the value of $a$, called a modal parameter. For a topological classification we have to consider only 4 parameters although for a differentiable classification 5 parameters are necessary. Thus $g$ has topological codimension 4 and differentiable codimension 5. For a more detailed discussion of topological and differentiable codimension see ([2], ch. IV §1 and ch. V §6).

We want to describe the bifurcation diagrams arising in (2) for different choices of the parameters $a$ and $\alpha_i$, $i=1,...,4$. A point $A=(a,\alpha_1,\alpha_2,\alpha_3,\alpha_4)$ in parameter space gives rise to a persistent bifurcation diagram if there is a neighbourhood of $A$ in parameter space where all bifurcation diagrams are equivalent to the bifurcation diagram of $A$. The sources of nonpersistence are the transition varieties $\mathcal{B}$, $\mathcal{H}$ and $\mathcal{D}$ denominated Bifurcation, Hysteresis and Double Limit respectively ([2], ch. III §5). The transition set, $\Sigma=\mathcal{B}\cup\mathcal{H}\cup\mathcal{D}$, divides the space of the unfolding parameters into connected components containing one of the persistent perturbations of (1). In the case of this modal family we are treating transition varieties are hypersurfaces in $\mathbb{R}^5$, which renders impracticable the enumeration of the connected components of $\mathbb{R}^5-\Sigma$.

In order to obtain an enumeration of the perturbed bifurcation diagrams of $g$, as well as an identification of the regions of the universal unfolding parameters space to which they belong, we are going to resort to path formulation. Path formulation ([2], ch. III §12) relates one state variable bifurcation problem with a path through the universal unfolding of a function.

In the next section we describe how we use the path formulation to identify the bifurcation problem $g$ with a path in the parameter space of the universal unfolding of the function $x^4$. Then we explain how we use the possible paths to construct the bifurcation diagrams in the unfolding of the modal family. The different types of local bifurcation found in this problem are presented in Section 3 in the form of a dictionary. In Section 4 transition varieties and bifurcation diagrams for (2) are presented in the $(\alpha_3,\alpha_2,\alpha_1)$-subspace of the unfolding parameter space.

## 2 – Path formulation

In order to relate the universal unfolding of $g$ to the universal unfolding of $x^4$,

$$x^4 + A\,x^2 + B\,x + C\ , \tag{3}$$

we fix $\varepsilon = 1$ and rewrite the former as

$$\begin{aligned} G(x,\lambda,\alpha_1,\alpha_2,\alpha_3,\alpha_4)\ &=\\ &= \ \varepsilon\,x^4 + (2\,a\,\lambda + \alpha_3)\,x^2 + (\alpha_2 + \alpha_4\,\lambda)\,x + (\alpha_1 + \delta\,\lambda^2)\ . \end{aligned} \tag{4}$$

We identify our bifurcation problem with a path

$$\lambda \to \Big(A(\lambda), B(\lambda), C(\lambda)\Big) \tag{5}$$

in the space of the parameters of the versal unfolding of $x^4$, by defining the functions

$$\begin{aligned} A(\lambda) \ &= \ 2\,a\,\lambda + \alpha_3\ ,\\ B(\lambda) \ &= \ \alpha_2 + \alpha_4\,\lambda\ ,\\ C(\lambda) \ &= \ \alpha_1 + \delta\,\lambda^2\ . \end{aligned} \tag{6}$$

Let $M$ be the surface in the 4-dimensional space $(x,A,B,C)$ defined by

$$M\colon\quad x^4 + A\,x^2 + B\,x + C \ = \ 0\ , \tag{7}$$

and let $m$ be the points of $M$ that have vertical tangent

$$m \ = \ \Big\{(x,A,B,C)\colon\ x^4 + A\,x^2 + B\,x + C \ = \ 0 \ \wedge \ 4\,x^3 + 2\,A\,x + B \ = \ 0\Big\}\ . \tag{8}$$

We define $\pi(m)$ as the projection of $m$ into the 3-dimensional space $(A,B,C)$ as follows

$$\pi(m) = \Big\{(A,B,C)\colon \exists\,x\colon\ x^4 + Ax^2 + Bx + C = 0 \ \wedge \ 4\,x^3 + 2\,Ax + B = 0\Big\}\ . \tag{9}$$

The variety $\pi(m)$, called swallowtail ([1], [4]), is shown in Figure 1. It has a curve of self-intersections and two curves of cusp points. For ease of reference we are going to call the part of the swallowtail below the line of self-intersections the pocket and the rest the tail.

The swallowtail divides $(A, B, C)$-space in regions where the number of zeros in the unfolding of $x^4$ is constant. Figure 1 shows the number of zeros in each region, see also Bröcker and Lander ([1], ch. 17).

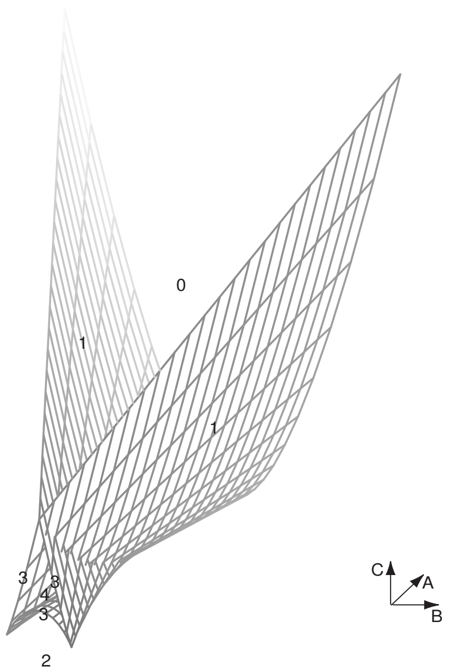


**Fig. 1 :** The swallowtail $\pi(m)$: projection into $(A, B, C)$-space of the points where the hypersurface $M : x^4 + Ax^2 + Bx + C = 0$ has a vertical tangent. The swallowtail divides the space in three components where the unfolding of $x^4$ has 4, 2 or 0 roots as indicated. On $\pi(m)$ the unfolding may have 1 or 3 roots in the points indicated, or 2 roots on the creased points at the pocket — see also Figure 2.

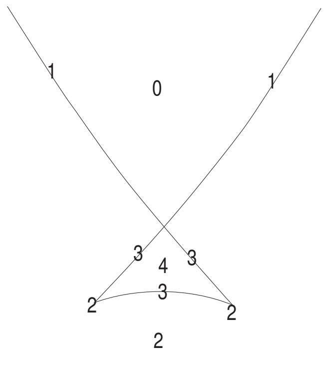


**Fig. 2 :** Intersection of $\pi(m)$, Figure 1, with the plane $A = \alpha$, where $\alpha$ is a negative constant, indicating the number of zeros of the unfolding of $x^4$ in each region.

Each bifurcation diagram is found by observing regions in $(A, B, C)$-space crossed by the path. Every time the path intersects the swallowtail surface there is a change in the number of branches.

The curve (5) is always a parabola in $(r, C)$-plane, where $r$ is a line in the $(A, B)$-plane. Consequently, the surfaces $M$ and $\pi(m)$ can be more easily visualized if instead of working directly with the surface of the swallowtail, we work with its intersection with vertical $(r, C)$-planes. We consider those vertical planes that give rise to different curves when intersected with the swallowtail.

In Figure 3 we show the projection into $(A, B)$-plane of the curves of cusp points of the swallowtail, as well as the different lines $r$ considered. The intersection of the swallowtail with each plane defined by one of those lines is presented in Figure 4. The swallowtail is symmetric under reflection in the $(A, C)$-plane. Therefore its intersection with symmetric planes gives rise to identical transition varieties and symmetric bifurcation diagrams, that are not considered here.

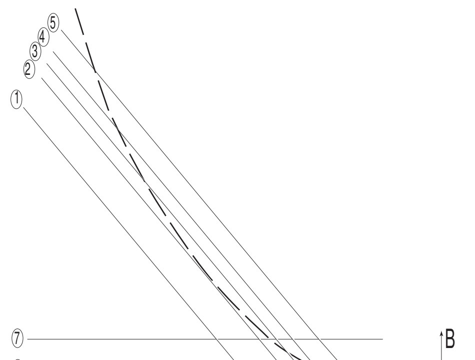


**Fig. 3 :** Lines in $(A, B)$-plane defining the vertical planes containing the parabolas (5). Dashed line: projection of the two curves of cusp points in $\pi(m)$.

From now on we refer to the intersection of the swallowtail with the vertical plane containing the $i^{\text{th}}$-line as case $i$. Cases 4, 5 and 7 give rise to identical intersections.

The case $A(\lambda) = constant$ is not considered here. It corresponds to one of the special values of the modal parameter $a$, $a = 0$, (see (6)) and thus to the bifurcation problem $g(x, \lambda) = x^4 + \delta\, \lambda^2$ that has infinite codimension.

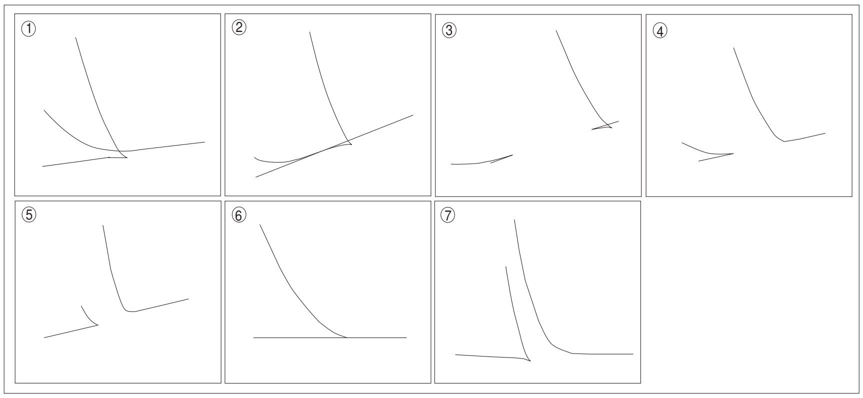


**Fig. 4:** Intersection of $\pi(m)$ with the planes defined by the lines in Figure 3.

Solving $A(\lambda) = 2\,a\,\lambda + \alpha_3$ for $\lambda$ we can write the parabolas (6) in $A$-parametrized form for $a \neq 0$:

$$
\begin{cases}
\lambda = \dfrac{A - \alpha_3}{2\,a} , \\[2ex]
B(A) = \alpha_2 + \alpha_4 \dfrac{A - \alpha_3}{2\,a} , \\[2ex]
C(A) = \alpha_1 + \dfrac{\delta}{4\,a^2} (A - \alpha_3)^2 .
\end{cases}
\tag{10}
$$

Each parabola lies in the vertical plane containing the line defined by the second equation. These lines are described by an equation of the form:

$$
B = k\,A + p , \tag{11}
$$

with $k$ and $p$ given by

$$
k = \frac{\alpha_4}{2\,a} \quad \text{and} \quad p = \alpha_2 - \frac{\alpha_3\,\alpha_4}{2\,a} . \tag{12}
$$

The case $B = constant$ is equivalent to $\alpha_4 = 0$ and $\alpha_2 = constant$. In the remaining cases we can write $\alpha_2$ as a function of $\alpha_3$, $\alpha_2 = k\,\alpha_3 + p$. In this study we established the value 1 for $\delta$, which implies that the parabolas have the concavity turned up. We do not consider the parabolas with the concavity turned down, that correspond to the case $\delta = -1$.

When $A$ tends to $-\infty$ the graph of the parabolas with opening less than $\frac{1}{4}$ is located in the interior of the swallowtail pocket and the graph of the parabolas with opening greater than $\frac{1}{4}$ is located in the region above the tail of the swallowtail. Therefore these paths give rise to bifurcation diagrams that possess respectively four and no zeros when $\lambda \to -\infty$. The opening of the parabola is determined by the value of the parameter $a$ and we consider parabolas with opening less than $\frac{1}{4}$, which implies $|a| > 1$.

The paths can be traced from left to right or vice-versa, originating bifurcation diagrams symmetric in relation to the vertical axis. We are going to consider the case where the paths are traced from left to right, which is equivalent to considering $a < 0$. This, together with the previous condition on $a$, means that $a < -1$.

## 3 – Dictionary

In this section we enumerate the types of bifurcation found in the unfolding of the modal family. We indicate instances where each type of bifurcation diagram occurs, that is which cases and which paths originate the diagram.

We start with local bifurcation problems of codimension less than or equal to 3 ([2], ch. IV §4, [3]). Then we discuss Double Limit points and finally tangencies and transversal crossing of transition varieties. We represent the zeros of each bifurcation problem in a bifurcation diagram with $\lambda$ in the horizontal axis and $x$ in the vertical axis.

Bifurcation diagrams are found by inspection of the relative positions of the intersection of each case $i$ and a parabola. The intersection of these two curves in the plane containing the parabola is sometimes so intricate that it is more easily understood in a deformed representation of the parabola.

### 3.1. Bifurcation problems of codimension 1 to 3

Chapter IV of [2] is dedicated to the study and classification of all local bifurcation problems of codimension less than or equal to three in one state variable. Such singularities are called elementary bifurcation problems. Most of these problems have a name, the rest will be identified by the numbers in [2]. The graphs of the transition varieties and the graphs of the persistent perturbed bifurcation diagrams of the elementary bifurcation problems are listed in ([2], ch. IV §4).

In [3] bifurcation problems of codimension up to seven with one state variable are classified. This classification includes a description of the subordination relations between those singularities. Given two bifurcation problems $g$ and $h$, we say that $g$ is *subordinate* to $h$ if $g$ is equivalent to a germ in the universal unfolding of $h$. If two singularities are related by subordination, they are called *adjacent*.

In Figure 5 we transcribe the part of Figure 1 of [3] which represents the subordination relations between some of the problems of codimension less than or equal to 5. Each line segment represents an adjacency, and indicates that the singularity of lower codimension is subordinated to that of higher codimension.

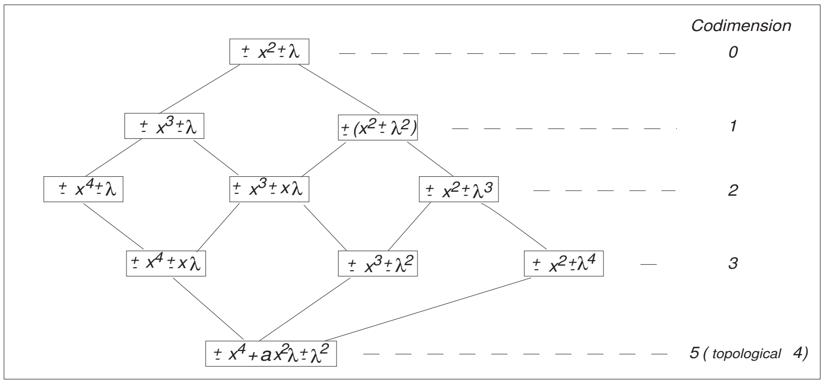


**Fig. 5 :** Subordination relations between the bifurcation problems subordinated to the modal familiy in study with height indicating codimension.

According to [3], except for singularities subordinated to modal singularities, each subordination relation between singularities of codimension less than eight can be realized through subordinations between bifurcations of consecutive codimension. In the case of our modal family, as it has topological codimendion 4 even though the codimension is 5, the germs of highest codimension in its unfolding are those of codimension 3.

The bifurcation problems subordinated to the modal family $g$ are Limit point, Simple bifurcation, Isola center, Hysteresis, Asymmetric cusp, Pitchfork, Quartic fold, Bifurcation problem number 8, Winged cusp and Bifurcation problem number 10.

A universal unfolding of the Bifurcation problem number 10 is given by $x^4 - \lambda x + \alpha + \beta\lambda + \gamma x^2$ ([2], ch. IV §4). When $\gamma < 0$ the graph of the transition set in the $(\alpha, \beta)$-plane presents symmetry in relation to the $\alpha$-axis.

We present the bifurcation diagrams in $\beta > 0$. The remaining bifurcation diagrams appear when we intersect the swallowtail with planes symmetric to those considered here.

The following is a list of how bifurcations are created.

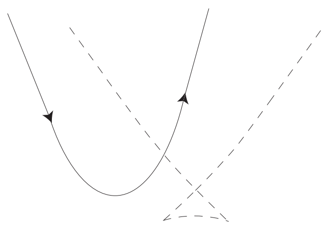

**Fig. 6:** Simple limit point arises from paths intersecting the swallowtail transversely at a regular point.

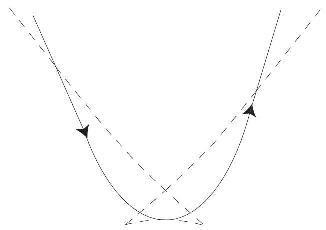

**Fig. 7:** Simple bifurcation, ([2], ch. IV §4), arises from paths tangent to the posterior part of the swallowtail pocket.

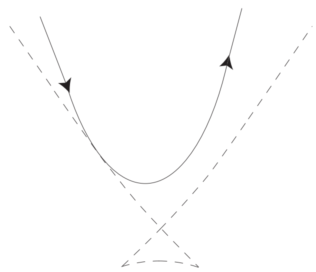

**Fig. 8:** Isola center, ([2], ch. IV §4), arises from paths tangent to the swallowtail at any points not in the posterior part of its pocket.

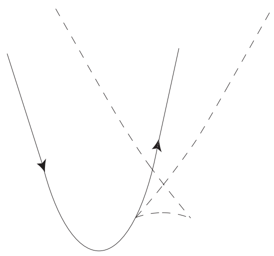

**Fig. 9:** Hysteresis, ([2], ch. IV §4), arises from paths through one of the cusp points of the swallowtail.

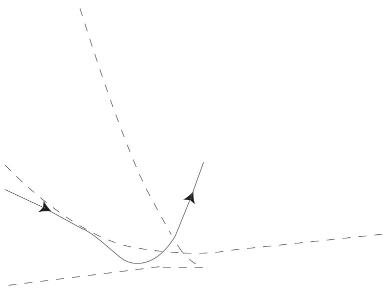

**Fig. 10 :** Asymmetric Cusp, ([2], ch. IV §4), arises from paths like this one and of its perturbations.

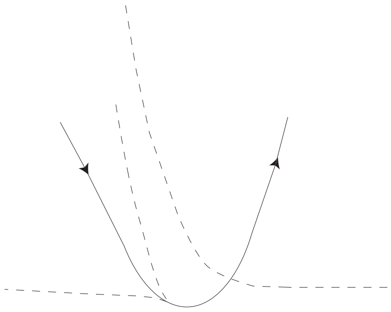

**Fig. 11 :** Pitchfork, ([2], ch. IV §4), only occurs in case 7 and arises from paths crossing the swallowtail at a cusp point like this one.

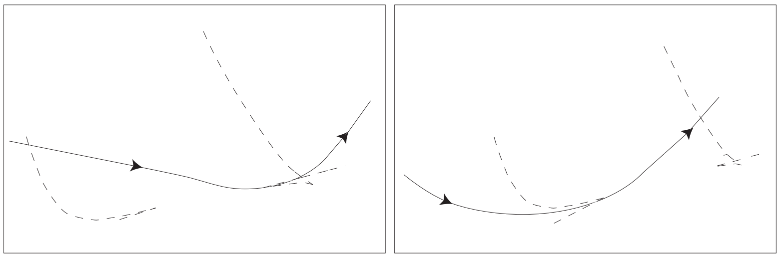

**Fig. 12 :** Winged cusp, ([2], ch. IV §4), with universal unfolding $x^3+\lambda^2+\alpha+\beta\,\lambda+\gamma\,x\,\lambda$, only appears in case 3. It arises from paths as those presented, respectively when $\gamma<0$ and $\gamma>0$.

Note that Quartic fold and Bifurcation problem number 8 are absent from this list because they have a different origin. These bifurcations arise when we move between two planes in Figure 3, that is, when we transform the intersecting parabola itself. We shall come back to this in Section 4.

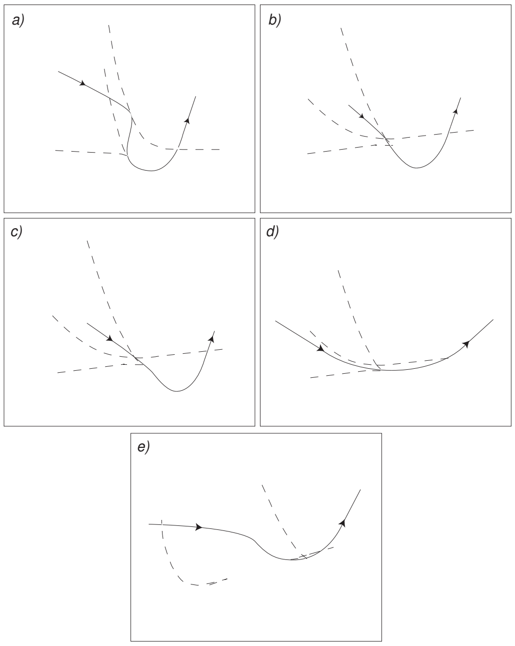


**Fig. 13 :** Example of paths that give rise, respectively, to
a) intersection of bifurcation with hysteresis,
b) tangency of bifurcation with double limit point,
c) intersection of hysteresis with double limit point,
d) intersection of bifurcation with hysteresis and
e) intersection of hysteresis with hysteresis,
that occur in the universal unfolding of the bifurcation problem number 10.

### 3.2. Global bifurcations

The simplest global bifurcation is the Double Limit, the only non-local type of generic point in the transition varieties.

We find transverse crossings of all the transition varieties, with the exception of the crossing of two Double Limit lines. This crossing corresponds to the existence of four double zeros and we have already seen that in the problem under consideration there are at most four simple zeros. The intersection of Bifurcation with Hysteresis happens in case 7, the tangency of Bifurcation with Double Limit, the intersection of Hysteresis with Double Limit and the intersection of Bifurcation with Hysteresis occur in cases 1, 2 and 3, and the intersection of Hysteresis with Hysteresis only happens in case 3.

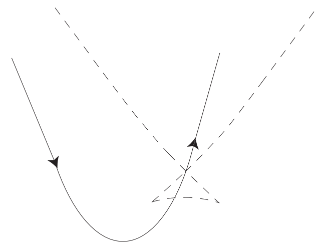

**Fig. 14 :** Double limit points arise from paths crossing the swallowtail at its line of self-intersections.

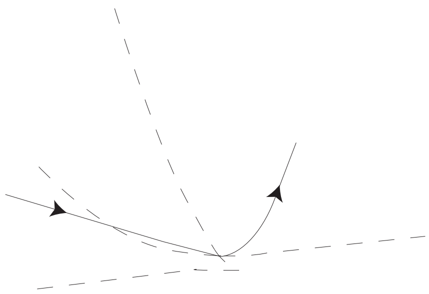

**Fig. 15 :** Tangency between Bifurcation and Double limit points, is found in cases 1, 2 and 3 and arises from paths like this.

## 4 – The modal family

We return to the discussion of bifurcation diagrams of $g(x, y)$ obtained from the intersection of a parabola with the swallowtail.

From the second equation in (10) it follows that the parameters $\alpha_2$ and $\alpha_4$ define the position of the plane containing the parabola, whereas the parameters $\alpha_1$ and $\alpha_3$ induce, respectively, horizontal and vertical translations of the parabola within this plane.

For each case $i$ we sketch in $(\alpha_1, \alpha_3)$-plane the relative positioning of the transition lines. We also show the persistent bifurcation diagrams, discussed in Section 3, corresponding to each region. We use thin dashed lines for Simple bifurcation, bold dashed lines for Isola center, thin solid lines for Hysteresis and bold solid lines for Double Limit.

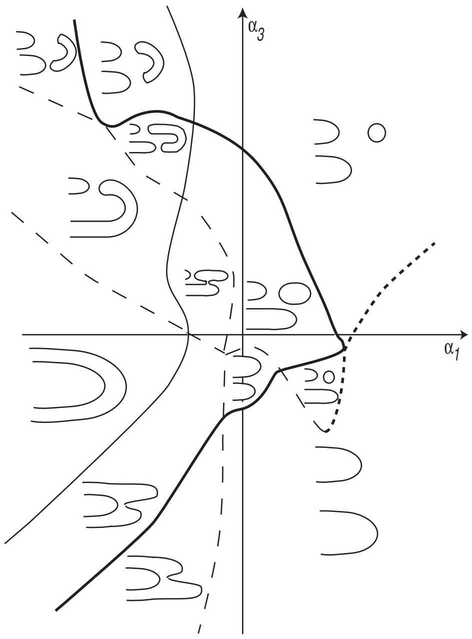


**Fig. 16 :** Case 1 – Sketch of the transition lines and persistent bifurcation diagrams in the $(\alpha_1, \alpha_3)$-plane. Conventions for the transition lines in the text.

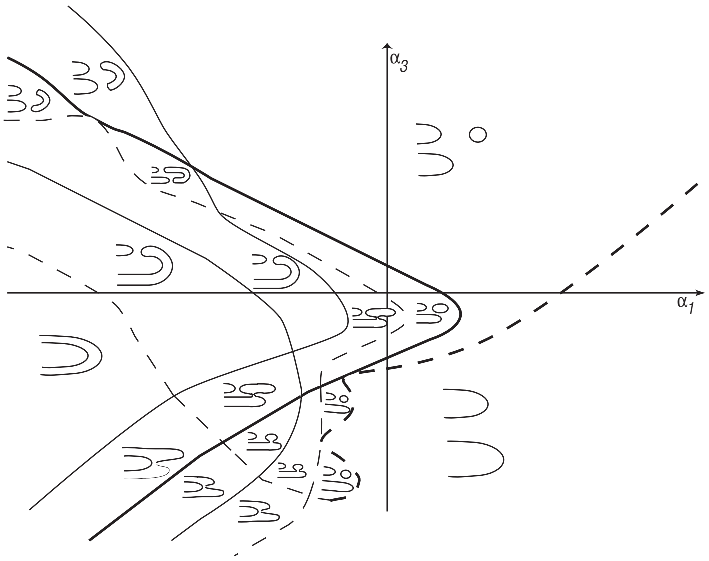


**Fig. 17 :** Case 2 – Sketch of the transition lines and persistent bifurcation diagrams in the $(\alpha_1, \alpha_3)$-plane. Conventions for the transition lines in the text.

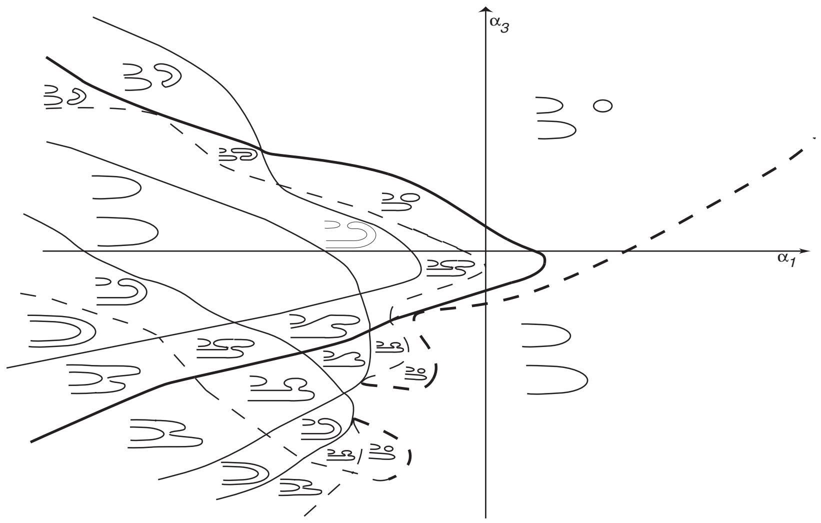


**Fig. 18 :** Case 3 – Sketch of the transition lines and persistent bifurcation diagrams in the $(\alpha_1, \alpha_3)$-plane. Conventions for the transition lines in the text.

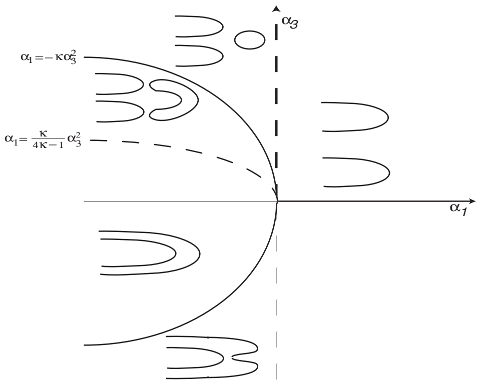


**Fig. 19 :** Case 6 – Sketch of the transition lines and persistent bifurcation diagrams in the $(\alpha_1, \alpha_3)$-plane. Conventions for the transition lines in the text.

Let $\Delta$ be the projection of the transition set in the $(\alpha_1, \alpha_2, \alpha_3)$-subspace of parameter space. Each plane containing a parabola is parallel to the $C$-axis and contains a line $B = k\,A + p$. As we have seen in Section 2, when $B = k\,A + p$ we have $\alpha_2 = k\,\alpha_3 + p$, i.e., in the 3-dimensional subspace $(\alpha_1, \alpha_2, \alpha_3)$ we have a plane parallel to the $\alpha_1$-axis that contains a line $\alpha_2 = k\,\alpha_3 + p$.

To imagine the surface $\Delta$ it is suficient to make the connection between the $(\alpha_1, \alpha_3)$-planes found for each case $i$ appealing to Figure 3 and to the correspondence between the lines $B = k\,A + p$ and the lines $\alpha_2 = k\,\alpha_3 + p$.

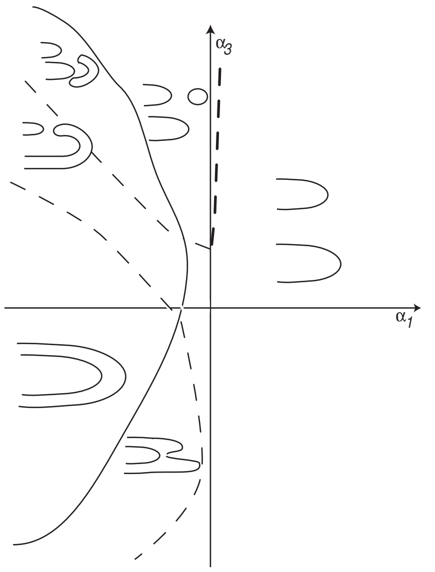


**Fig. 20 :** Case 7 – Sketch of the transition lines and persistent bifurcation diagrams in the $(\alpha_1, \alpha_3)$-plane. Conventions for the transition lines in the text.

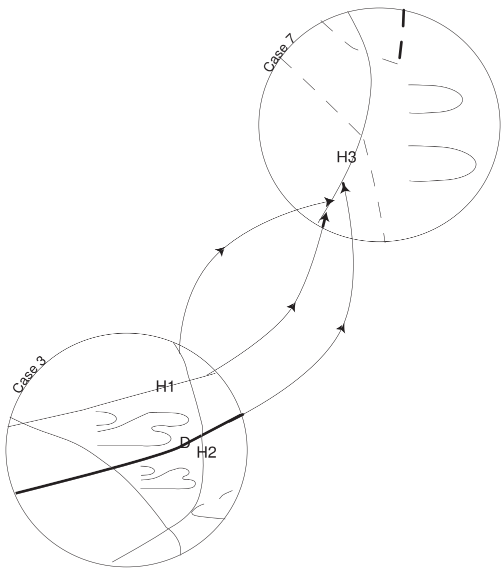


**Fig. 21 :** Region in $(\alpha_1, \alpha_3)$-plane of case 3 and region in $(\alpha_1, \alpha_3)$-plane of case 7 (analogous to that of case 4) in which connection appears the bifurcation problem Quartic fold. Arrows indicating that in the transition of case 3 to case 4 the transition lines H1, D and H2 become closer and closer until they join and give rise to the transition line H3.

We are now able to find the bifurcation problems Quartic fold and number 8 in the versal unfolding of the modal family.

In the transition from case 3 to case 4 (which as we have seen is analogous to case 7) we find the bifurcation problem Quartic fold. In Figure 21 we show the region in $(\alpha_1, \alpha_3)$-plane of case 3 and the region in $(\alpha_1, \alpha_3)$-plane of case 7 in which connection appears the bifurcation problem Quartic fold. For a better understanding let us observe Figure 3 again and let us consider lines of type 3 closer and closer of the line of type 4. When we make this approach the transition lines identified in Figure 21 as H1, D and H2 become closer and closer, until when we move to line of type 4 those transition lines join and originate the transition line identified H3 in Figure 21, according to the arrows.

In Figure 22 we represent, in the parameter space $(\beta, \gamma, \alpha)$, the universal unfolding of the bifurcation problem number 8. Let us consider the intersection of Figure 22 with planes parallel to the $\alpha$-axis defined by lines $\gamma = k\,\beta + p$ and $\beta = 0$ with $k \geq 0$.

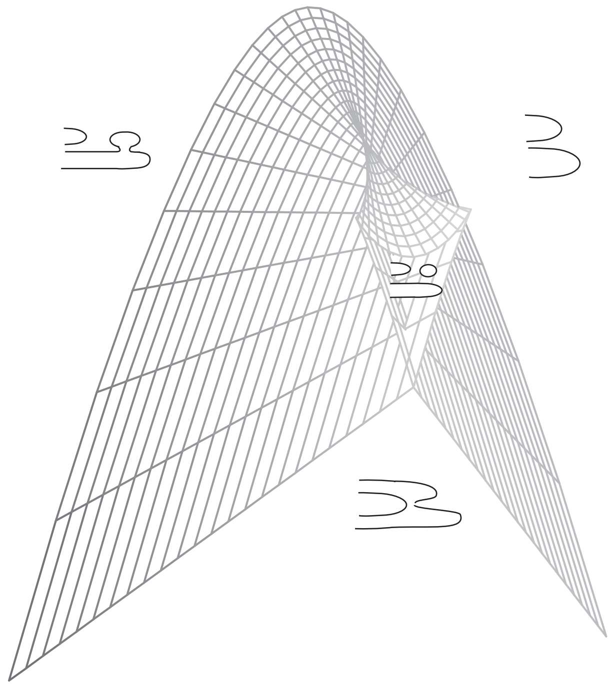

**Fig. 22:** Universal unfolding in parameter space $(\beta, \gamma, \alpha)$ of the bifurcation problem number 8.

In Figure 23 we show the different results of these intersections. We draw attention to the fact that intersection 2 is the result of intersecting Figure 22 with a plane tangent to one of the curves of cusp points of the Bifurcation variety of problem number 8, and intersection 5 results of intersecting Figure 22 with the plane defined by $\beta = 0$.

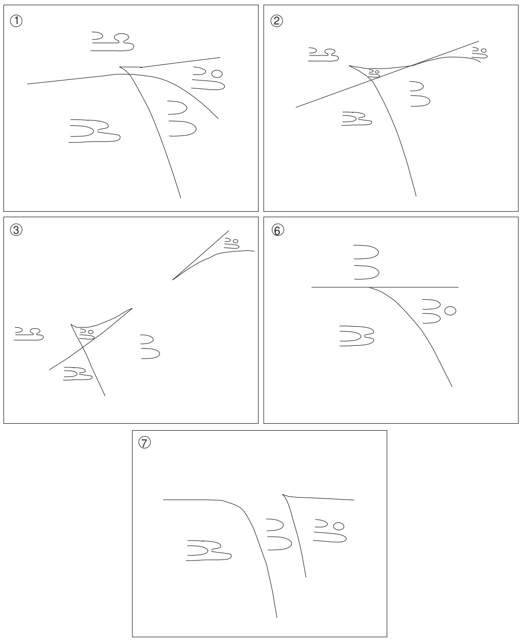

**Fig. 23:** Different intersections of Figure 7 with planes parallel to the $\alpha$-axis defined by lines $\gamma = k\,\beta + p$ and $\beta = 0$ with $k \geq 0$.

Note that each intersection $i$ is identified with a region in the $(\alpha_1, \alpha_3)$-plane of case $i$. This is not totally true in what concerns intersection 1 and case 1. What happens in case 1 is that the region in the $(\alpha_1, \alpha_3)$-plane that contains intersection 1 suffers the action of the passage of a Double Limit line. So, what we find in that region is not properly intersection 1 but its result after the action of a Double Limit, see Figure 24.

Furthermore, the line that gives origin to case $i$ and the line that gives origin to intersection $i$ represent the same line, respectively, in the $(A, B)$-plane and in the $(\beta, \gamma)$-plane.

This way we prove that bifurcation problem number 8 is subordinated to the modal family $g$, as promised.

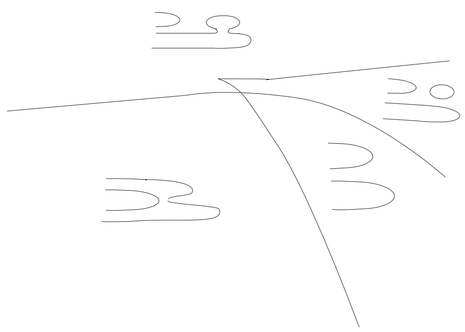

**Fig. 24 :** Intersection 1 (Figure 8) after the action of a Double limit.

*ACKNOWLEDGEMENTS* – The first author benefitted from funding from Action 5.2 of PRODEP, grant 3/98. The last two authors benefitted from funding from Fundação para a Ciência e Tecnologia, Portugal, grant 2/2.1/MAT/407/94 of programme PRAXIS XXI and Centro de Matemática Aplicada da Universidade do Porto, Portugal.

## REFERENCES

[**1**] Brocker, Th. and Lander, L. – *Differentiable Germs and Catastrophes*, London Mathematical Society Lecture Notes Series, 17, Cambridge University Press, 1975.

[**2**] Golubitsky, M. and Schaeffer, D.G. – *Singularities and Groups in Bifurcation Theory*, vol. I, Springer-Verlag, 1985.

[**3**] Keyfitz, B.L. – *Classification of one-state-variable bifurcation problems up to codimension seven*, in "Dynamics and Stability of Systems", vol. 1, pp. 2–41, 1986.

[**4**] Poston, T. and Stewart, I. – *Catastrophe Theory and its Applications*, Pitman, 1978.

Manuela A.D. Aguiar and Sofia B.S.D. Castro,
Faculdade de Economia, Universidade do Porto,
Rua Dr. Roberto Frias, 4200 Porto – PORTUGAL
E-mail: maguiar@fep.up.pt
sdcastro@fep.up.pt

and

Sofia B.S.D. Castro and Isabel S. Labouriau,
Centro de Matemática Aplicada, Universidade do Porto,
Rua das Taipas, 135, 4050-600 Porto – PORTUGAL

and

Isabel S. Labouriau,
Departamento de Matemática Aplicada, Faculdade de Ciências, Universidade do Porto,
Rua das Taipas, 135, 4050-600 Porto – PORTUGAL
E-mail: islabour@fc.up.pt